Research in Pharmaceutical Sciences, December 2023; 18(6): 626-637
Received: 15-01-2023
Peer Reviewed: 17-03-2023
Revised: 12-06-2023
Accepted: 26-08-2023
Published: 23-11-2023

School of Pharmacy & Pharmaceutical Sciences
Isfahan University of Medical Sciences

Original Article

Computational design of newly engineered DARPins as HER2 receptor inhibitors for breast cancer treatment

Maryam Beheshti Isfahani[1], Karim Mahnam[2,*], Hooria Seyedhosseini-Ghaheh[3,*], Hamid Mir Mohammad Sadeghi[1], Hossein Khanahmad[4], Vajihe Akbari[1], and Jaleh Varshosaz[5]

[1]Department of Pharmaceutical Biotechnology, School of Pharmacy and Pharmaceutical Sciences, Isfahan University of Medical Sciences, Isfahan, Iran.
[2]Faculty of Science, Department of Biology, Shahrekord University, Shahrekord, Iran.
[3]Nutrition and Food Security Research Center, Isfahan University of Medical Sciences, Isfahan, Iran.
[4]Department of Genetics and Molecular Biology, School of Medicine, Isfahan University of Medical Science, Isfahan, Iran.
[5]Novel Drug Delivery Systems Research Center, Department of Pharmaceutics, School of Pharmacy and Pharmaceutical Sciences, Isfahan University of Medical Sciences, Isfahan, Iran.

Abstract

Background and purpose: Human epidermal growth factor receptor 2 (HER2) is overexpressed in approximately 25% of breast cancer patients; therefore, its inhibition is a therapeutic target in cancer treatment.
Experimental approach: In this study, two new variants of designed ankyrin repeat proteins (DARPins), designated EG3-1 and EG3-2, were designed to increase their affinity for HER2 receptors. To this end, DARPin G3 was selected as a template, and six-point mutations comprising Q26E, I32V, T49A, L53H, K101R, and G124V were created on its structure. Furthermore, the 3D structures were formed through homology modeling and evaluated using molecular dynamic simulation. Then, both structures were docked to the HER2 receptor using the HADDOCK web tool, followed by 100 ns of molecular dynamics simulation for both DARPins / HER2 complexes.
Findings/Results: The theoretical result confirmed both structures' stability. Molecular dynamics simulations reveal that the applied mutations on DARPin EG3-2 significantly improve the receptor binding affinity of DARPin.
Conclusion and implications: The computationally engineered DARPin EG3-2 in this study could provide a hit compound for the design of promising anticancer agents targeting HER2 receptors.

Keywords: Breast cancer; Designed ankyrin repeat proteins; Docking; Molecular dynamic simulation.

INTRODUCTION

Breast cancer is the most prevalent malignancy in women and one of this group's leading causes of mortality (1). Human epidermal growth factor receptor 2 (HER2) overexpression is a prognostic marker in 20 to 25% of breast cancer and gastroesophageal cancer patients; inhibition of the HER2 receptor is an established therapeutic target (2,3). Tumor targeting with peptide aptamers (PAs) is a well-established method for treating cancer; PAs are small combinatorial scaffolds with specific binding to precise sites on their targets.

Designed ankyrin repeat proteins (DARPins) are one of the classes of PAs introduced by Plückthun *et al.* in 2003, representing a group of highly stable, small-sized binding proteins based on a repeat protein scaffold (4,5).

*Corresponding authors:
K. Mahnam, Tel: +98-384424402, Fax: +98-3832324419
Email: mahnam.karim@sci.sku.ac.ir
H. Seyedhosseini-Ghaheh , Tel: +98-3137923164, Fax: +98-3136681378
Email: h.hosseini@nutr.mui.ac.ir

Access this article online
Website: http://rps.mui.ac.ir
DOI: 10.4103/1735-5362.389950

PAs are utilized in numerous direct detection procedures and have found various uses in therapeutic targeting due to their robustness and simplicity. DARPin G3 has a high affinity for HER2 (4,5). In addition, DARPin F1, the most improved variant with nine mutations throughout the maturation process, showed an almost 700-fold increase in affinity compared to its parent (6). Moreover, the rational design of DARPins allows them to effectively induce apoptosis in HER2-dependent breast cancer cell lines (7,8).

Novel clinical treatments based on HER2, downstream effectors, and compensatory signaling pathways are currently being developed (5). The pro-apoptotic Bcl-2-associated X protein (BAX) protein is the most potent apoptosis promoter, which induces tumor cell death. Recent reports indicate that the second mitochondria-derived activator of caspase/direct inhibitor of apoptosis-binding protein with low pI (Smac/DIABLO) acts as a common mediator of the mitochondrial pathway and death receptor pathway of apoptosis in tumor cells (9,10). In addition, preclinical research demonstrated that Smac mimics affected direct cancer cell death or sensitized cancer cells to various cytotoxic therapies. Smac mimics the N-terminal four amino acid sequence (Ala-Val-Pro-Ile), which enables Smac to bind to inhibitors of apoptosis proteins (11-13).

Designing new DARPin variants with more affinity and stability in *Escherichia coli* will help therapeutic targeting. Due to the cost-effectiveness development of protein drugs, computational methods like *in silico* protein design, molecular dynamic (MD) simulation, and docking are prioritized to enhance their desired features (14,15).

In this study, a DARPin G3 (EG3-1; 360 amino acids) was engineered to bind to the HER2 receptor. Native DARPin G3 (residues 1-136; PDB code: 2jab) was bonded to a linker (residues 137-146) and a furin protease cutting position sequence (RHRQPRGWEQL) for this purpose (residue 147-158). These constituents were then attached to downstream effectors BAX and Smac/DIABLO (Uniprot cods: Q07812; residue 159-360).

The study by Houlihan *et (al*. on variants of DARPin revealed that the Q26E, I32V, T49A, L53H, K101R, and G124V mutations in native DARPin increased its affinity for the HER2 receptor by nearly 700-fold (6). To this end, we designed six-point mutations in the native structure of DARPin to increase its affinity for HER2. The final structure was characterized as EG3-2 (360 amino acids).

The comparison of these two structures using MD simulation can suggest the optimal structure for future experimental research and aid in developing novel therapeutically targeted proteins for the treatment of breast cancer.

METHODS AND DESIGN

Structural modeling of DARPin EG3-1 and EG3-2

The 3D structures of DARPin EG3-1 and EG3-2 were constructed in MODELLER v. 10 software using the structure of DARPin (PDB ID: 2jab) and the BAX and Smac/DIABLO proteins (Uniprot ID: Q07812). The modeler created one thousand models, and the model with the lowest discrete optimized protein energy (DOPE) score was selected as the optimal model. The selected models were evaluated using PROCHECK and ProSA-web (16,17). The ProSa-web statistics are provided in the supplementary materials (Fig. S1A and B).

MD simulations of DARPin EG3-1 and EG3-2

The G43a1 force field was used to conduct MD simulations with the GROMACS 2018 software (13). The water model's simple point charge was used to solvate the system (SPC216). With a cutoff distance of 10 Å, the long-range electrostatic interactions were modeled using the particle mesh Ewald method. DARPin EG3-1 and DARPin EG3-2 models were solvated in a solvation box with a 10 Å distance between the edges of the box and the protein surface. To this end, a triclinic box with periodic 3D boundary conditions was selected. Moreover, each system was neutralized by adding nine negative ions (Cl^-).

First, the energy of each system was minimized using the steepest descent and conjugate gradient algorithms to eliminate

steric hindrance caused by the addition of hydrogen atoms. In the subsequent step, known as the position restraint step, the linear constraint solver (LINCS) algorithm was utilized to constrain the hydrogen-containing bonds. Temperature and pressure were stabilized using a two-step position restraint procedure in conjunction with NVT (500 ps) and NPT (1000 ps) ensembles, the Berendsen algorithm, and a pressure coupling constant of 0.1 ps. Lastly, a 100-ns MD simulation of native DARPin at 310 K was performed. MD simulations utilized a 0.001 ps time step. The Nosé-Hoover thermostat was employed to fix the system's temperature, while the Parrinello-Rahman pressure coupling method was chosen to maintain the system's pressure at 1 atm. The final structure of native DARPin was then utilized to generate mutated DARPin or DARPin EG3-2, and MD simulations were performed under the same conditions.

Root mean square fluctuation (RMSF), root mean square deviation (RMSD), solvent accessible surface area (SASA), the radius of gyration (Rg), the number of hydrogen bonds between protein and solvent, and the number of secondary structure elements over the last 30 for both DARPin EG3-1 and EG3-2 were used to analyze the stability of protein structures and their interaction with the solvent.

MD simulation of the HER2 receptor

The structure of the HER2 extracellular domain (ECD) domain (PDB ID: 1n8z; chain C) was used for 20 ns MD simulation with the same previous conditions to investigate the interaction of the engineered DARPin and HER2 ECD domain. Ten Na^+ ions were added to neutralize each system. This simulation box contained 47836 water molecules.

Molecular docking of DARPin to the HER2 ECD receptor

The HADDOCK 2.4 web server (https://wenmr.science.uu.nl/haddock2.4/) was used to assess the interaction between DARPin EG3-1 and EG3-2 and the HER2 ECD domain. The residues 43-108 of DARPin EG3-1 and EG3-2 and 435-900 of the HER2 receptor were considered active residues during docking (18).

MD simulation of DARPin/ECD HER2 receptor complexes

The optimal complex of DARPin EG3-1 and EG3-2 with the HER2 receptor was identified using the HADDOCK server and used for MD simulation. To evaluate the interaction between DARPin EG3-1 and EG3-2 and the HER2 receptor, each complex underwent a 100-ns MD simulation. With the addition of 17 Cl^- ions and 46842 water molecules for EG3-1 and 19 Cl^- ions and 46715 water molecules for EG3-2, the HADDOCK-obtained complexes were subjected to a 100-ns MD simulation under the same conditions already described. UCSF Chimera 1.12 (https://www.cgl.ucsf.edu/chimera/download.html) was utilized to display the 3D structures of complexes (19-21).

RESULTS

Verification of models

According to the Ramachandran plot available on the PROCHECK web server (https://www.ebi.ac.uk/thornton-srv/software/PROCHECK/), 82.2% and 81.5% of residues of the optimal models of DARPin EG3-1 and DARPin EG3-2, respectively, were in the most favored regions and 3% of residues of DARPin EG3-1 and DARPin EG3-2 were in disallowed regions (Fig. 1 A and B).

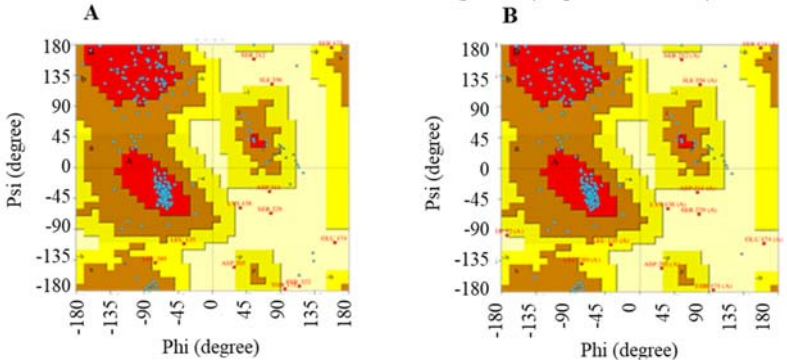

Fig. 1. The Ramachandran plot of the designed (A) DARPin EG3-1 and (B) DARPin EG3-2. DARPin EG, Designed ankyrin repeat proteins engineered G.

DARPin EG3-1 and DARPin EG3-2 exhibited Z scores of -9.17 and -3.67, respectively, according to ProSA-web (https://prosa.services.came.sbg.ac.at/prosa.php). The Z-score indicates the quality of the model as a whole and measures the deviation of the structure's total energy concerning energy dispersion caused by random conformations. These values are consistent with typical Z-scores for a 400-residue protein. Prosa-web Z-score plots of the optimal models are provided in the supplementary materials (Fig. S1).

MD simulations and output analyses of DARPin EG3-1 and DARPin EG3-2

Two designed variants were subjected to additional structural and dynamic analyses using MD simulations. Based on the backbone's RMSD, all structures reached a stable state after approximately 30 ns (Fig. 2A and Table 1). Then, dynamic parameters for each structure during the final 30 ns of the simulation were computed (Table 1).

The greater backbone RMSD of DARPin EG3-2 compared to native DARPin was due to substantial changes in protein structure caused by the DARPin EG3-1 mutation.

Local structural fluctuations plot or RMSF plot (Fig. 2B) during the final 30 ns MD simulation demonstrated that the flexibility of residues in DARPin EG3-2 is lower than in DARPin EG3-1, particularly in the BAX domain (residue 159-360).

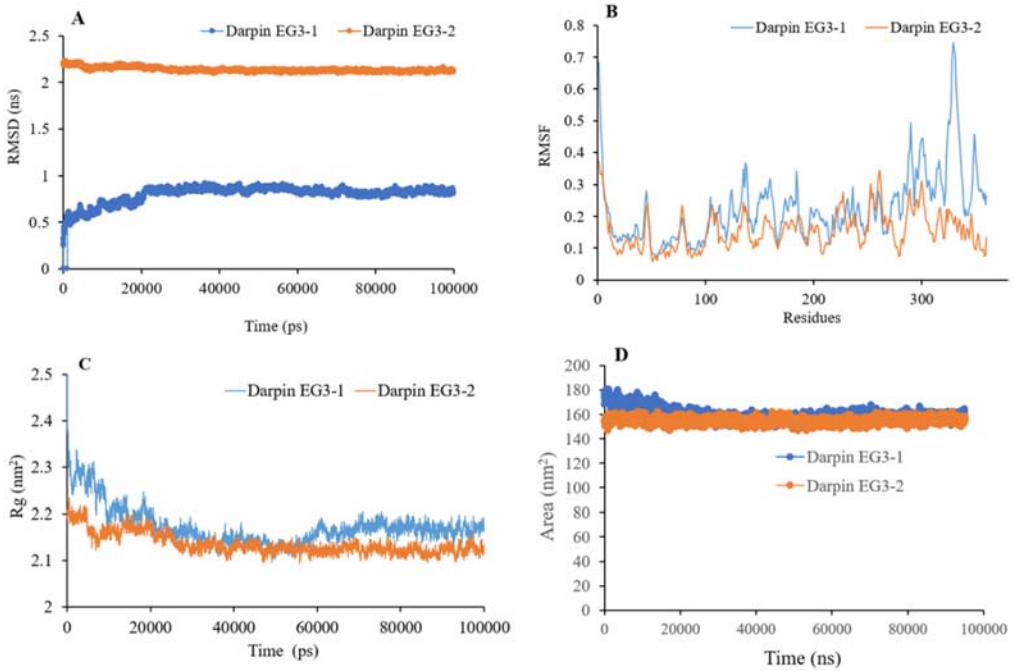

Fig. 2. Molecular dynamic simulation results of the DARPin EG3-1 variant compared with the DARPin EG3-2 during 100 ns. Plots illustrate (A) RMSD, (B) RMSF, (C) Rg, and (D) solvent-accessible surface area trends for the DARPin EG3-1 and DARPin EG3-2. DARPin EG, Designed ankyrin repeat proteins engineered G; RMSD, root mean square deviation; RMSF, root mean square fluctuation; Rg, radius of gyration.

Table 1. The average molecular dynamic simulation parameters for DARPin EG3-1 and DARPin EG3-2 during the last 30 ns and receptor during the last 5 ns. The data are presented as mean ± SD.

Parameters	EG3-1	EG3-2	Receptor
Root mean square deviation (nm)	0.85 ± 0.02	2.12 ± 0.01	0.74 ± 0.06
Root mean square fluctuation (nm)	0.225 ± 0.109	0.155 ± 0.059	0.09 ± 0.06
Radius of gyration (nm)	2.14 ± 0.01	2.12 ± 0.01	3.28 ± 0.06
Surface accessible solvent area (nm^2)	156 ± 2.16	154.68 ± 2.3	409.6 ± 4.6
The number of intramolecular hydrogen bonds (protein-protein)	247.51 ± 8.55	255.5 ± 8.73	658.6 ± 32.6
The number of intermolecular hydrogen bonds (protein-solvent)	590 ± 15.50	574.5 ± 16.73	1266 ± 60.6

DARPin EG, Designed ankyrin repeat proteins engineered G.

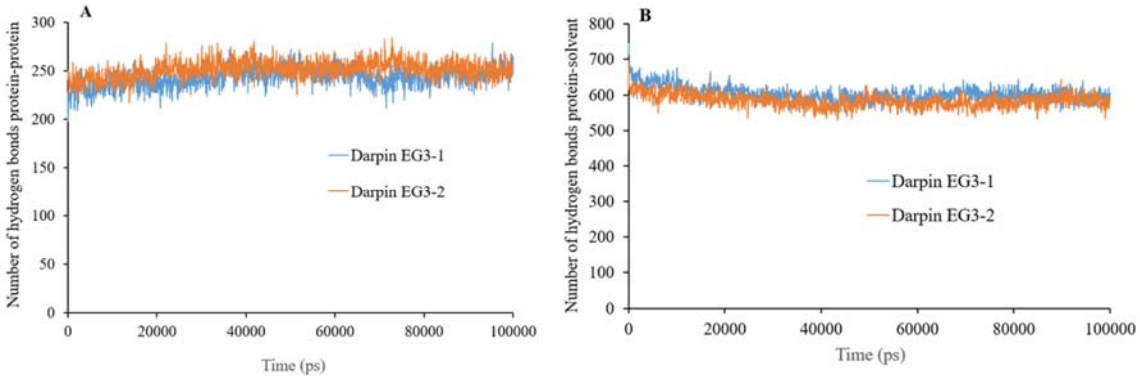

Fig. 3. Molecular dynamic simulation results of the DARPin EG3-1 variant compared with the DARPin EG3-2 during 100 ns. Plots illustrate (A) intramolecular (protein-protein) hydrogen bonds of DARPin EG3-1 and DARPin EG3-2 and (B) intermolecular (protein-solvent) hydrogen bonds of DARPin EG3-1 and DARPin EG3-2. DARPin EG, Designed ankyrin repeat proteins engineered G.

Table 2. The number of residues in secondary structural elements of DARPin EG3-1 and DARPin EG3-2 in their free and complex forms during the final 30 ns of molecular dynamics simulation.

Parameters	DARPin EG3-1	DARPin EG3-2	DARPin EG3-1 in Her2 complex	DARPin EG3-2 in Her2 complex
Structure	192.8	196.2	192.8	196.2
Coil	101.6	99.22	101.7	99.20
B-Sheet	4.190	5.650	4.190	5.650
B-Bridge	4.570	13.35	4.570	13.35
Bend	58.25	57.85	58.25	57.85
Turn	58.01	56.59	58.01	56.59
Helix	133.2	127.3	133.2	127.3

DARPin EG, Designed ankyrin repeat proteins engineered G.

Notably, the RMSF values of mutated residues such as Q26E, I32V, T49A, L53H, K101R, and G124V do not differ significantly between native and mutated DARPins. According to the Rg and SASA analysis, DARPin EG3-2 possesses more compact and intramolecular contacts than DARPin EG3-1. The decreased flexibility of DARPin EG3-2 was consistent with its reduced Rg and SASA (Fig. 2C and D) which might be related to the variant's increased stability.

Furthermore, to study the internal and external interaction of DARPin EG3-1 and DARPin EG3-2, the average number of intramolecular (protein-protein) and intermolecular (protein-solvent) hydrogen bonds were calculated for the last 30 ns of MD simulation (Table 1). Moreover, the hydrogen bonds within the protein structure and between the protein and solvent were plotted in Fig. 3A and B.

Moreover, the number of secondary structure elements in both DARPins was determined using the dictionary of secondary structures in proteins (DSSP) algorithm to detect specific patterns of hydrogen bonds between amino acid residues (Table 2).

HADDOCK results

The final structures of DARPin EG3-1 and DARPin EG3-2 obtained from 100 ns MD simulation was used for the docking step. According to the HADDOCK results, DARPin EG3-2 interacted with the ECD domain HER2 receptor more effectively than DARPin EG3-1 (Table 3). This suggests that the mutations increase DARPin's affinity for the HER2 receptor. Also, reported in dockings are electrostatic, van der Waals, desolation, and buried surface area energies (Table 3).

MD simulations of complexes

For each of the best complexes provided by the Haddock server, 100 ns of MD simulations were performed to provide additional structural information and dynamic studies. After 15 ns, the RMSD values of the HER2 receptor in both complexes of DARPin EG3-1 and DARPin EG3-2 stabilized. All the previously mentioned analysis was performed based on the parameters obtained from the second half of the simulations. In addition, the minimum distance between DARPins and the ECD of the HER2 receptor and the average number of contacts

(distances less than 6) between them was calculated (Table 4).

Hydrogen bonding is an exceptional form of dipole-dipole interaction between molecules. Despite having lower interaction energy (4 kJ to 50 kJ per mole of hydrogen bonds) than covalent bonding, the number of hydrogen bonds formed is essential for protein folding (18,19). In this study, the hydrogen bonds formed between the chains of DARPin EG3-1 and DARPin EG3-2 and the ECD of the HER2 receptor were analyzed, and the results are presented in Table 5.

Table 3. HADDOCK results. The data except for cluster size and Z-score are expressed as mean ± SD.

HADDOCK parameters	DARPin EG3-1 / HER2 complex	DARPin EG3-2 / HER2 complex
HADDOCK score	-126.1 ± 22.2	-142.7 ± 9.2
Cluster size	4	19
Root mean square deviation (Å)	0.6 ± 0.4	1.1 ± 0.9
Van der Waals energy (kcal mol^{-1})	-83.3 ± 20.4	-97.6 ± 14.2
Electrostatic energy (kcal mol^{-1})	-543.3 ± 63.6	-309.8 ± 72.5
Desolvation energy (kcal mol^{-1})	17.7 ± 6.6	-10.0 ± 8.9
Buried surface area ($Å^2$)	3106.1 ± 441.7	2897.2 ± 224.2
Z-Score	-2.4	-2.3

DARPin EG, Designed ankyrin repeat proteins engineered G; HER, human epidermal growth factor receptor.

Table 4. The average properties of two complexes during the last 50 ns of the molecular dynamic simulation. The data present mean ± SD.

The average parameters	DARPin EG3-1 / HER2	DARPin EG3-2 / HER2
RMSD of DARPin EG3 in complex (nm)	0.17 ± 0.01	0.17 ± 0.02
RMSD of HER2 receptor in complex (nm)	0.28 ± 0.03	0.71 ± 0.03
RMSF of DARPin EG3 in complex (nm)	0.12 ± 0.06	0.09 ± 0.03
RMSF of HER2 receptorin complex (nm)	0.1 ± 0.03	0.09 ± 0.05
Rg of DARPin EG3 in complex (nm)	2.15 ± 0.01	2.17 ± 0.01
Rg of HER2 receptor in complex (nm)	3.22 ± 0.02	3.05 ± 0.02
Sum of electrostatic and van der Waals energies between DARPin EG3 and HER2 receptor (kJ/mol)	-556.6	-392.3
The number of contacts between DARPin EG3 and HER2 receptor	630 ± 23.8	558 ± 19.2
The number of hydrogen bonds between DARPin EG3 and HER2 receptor	20 ± 3.8	14 ± 2.4

DARPin EG, Designed ankyrin repeat proteins engineered G; HER, human epidermal growth factor receptor; RMSD, root mean square deviation; RMSF, root mean square fluctuation; Rg, radius of gyration.

Table 5. The number and position of hydrogen bonds between DARPin EG3-1, DARPin EG3-2, and ECD in HER2 receptor complexes.

DARPin EG3-1		DARPin EG3-2	
Chian A (DARPin EG3-1)	**Chain B (ECD of HER2 receptor)**	**Chian A (DARPin EG3-2)**	**Chain B (ECD of HER2 receptor)**
Gln 109	Pro 901	His 102	Ser 484
Lys 101	Asp 522	His 5	Tyr 323
Gly 260	Asp 522	Asn 36	Leu 73
Gly 260	Asn 983	Gly 70	Arg 459
Lys 101	Asp 1	Asp 259	Tyr 308
Lys 43	Asp 895	Asn 107	His 454
Lys 43	Gln 896	Arg 101	Arg 515
Arg 235	Gln 905	Asp 110	Lys 444
Asp 110	Val 986	Ala 78	Lys 444
Arg 235	Arg 510	Asn 41	Met 457
Asp 255	Gln 945	His 9	Val 332
-	-	His 9	Ser 333
-	-	Glu 45	Tyr 366
-	-	His 10	Tyr 366
-	-	Lys 43	Arp 365
-	-	Lys 43	Thr 439
-	-	Lys 43	Asp 456

DARPin EG, Designed ankyrin repeat proteins engineered G; HER, human epidermal growth factor receptor; ECD, extracellular domain.

Figures 4 and 5 depicts the predicted complex binding mode of DARPin EG3-1 and DARPin EG3-2, as well as the position of hydrogen bonds and hydrophobic interactions between the ECD of the HER2 receptor and the active site residues of DARPin EG3-1 and DARPin EG3-2. This Figure was generated using the LigPlot program. The mutant form has a greater dispersion of hydrogen and hydrophobic bonds than the native form, resulting in a more stable structure. Significant changes have occurred in the number, distribution, length, and type of amino acids involved in hydrogen and hydrophobic bonds due to mutations in the mutant form (h-bond native and mutant). Figure 6 depicts the final 3D structure of the DARPin EG3-2/HER2 complex after 100 ns of MD simulation.

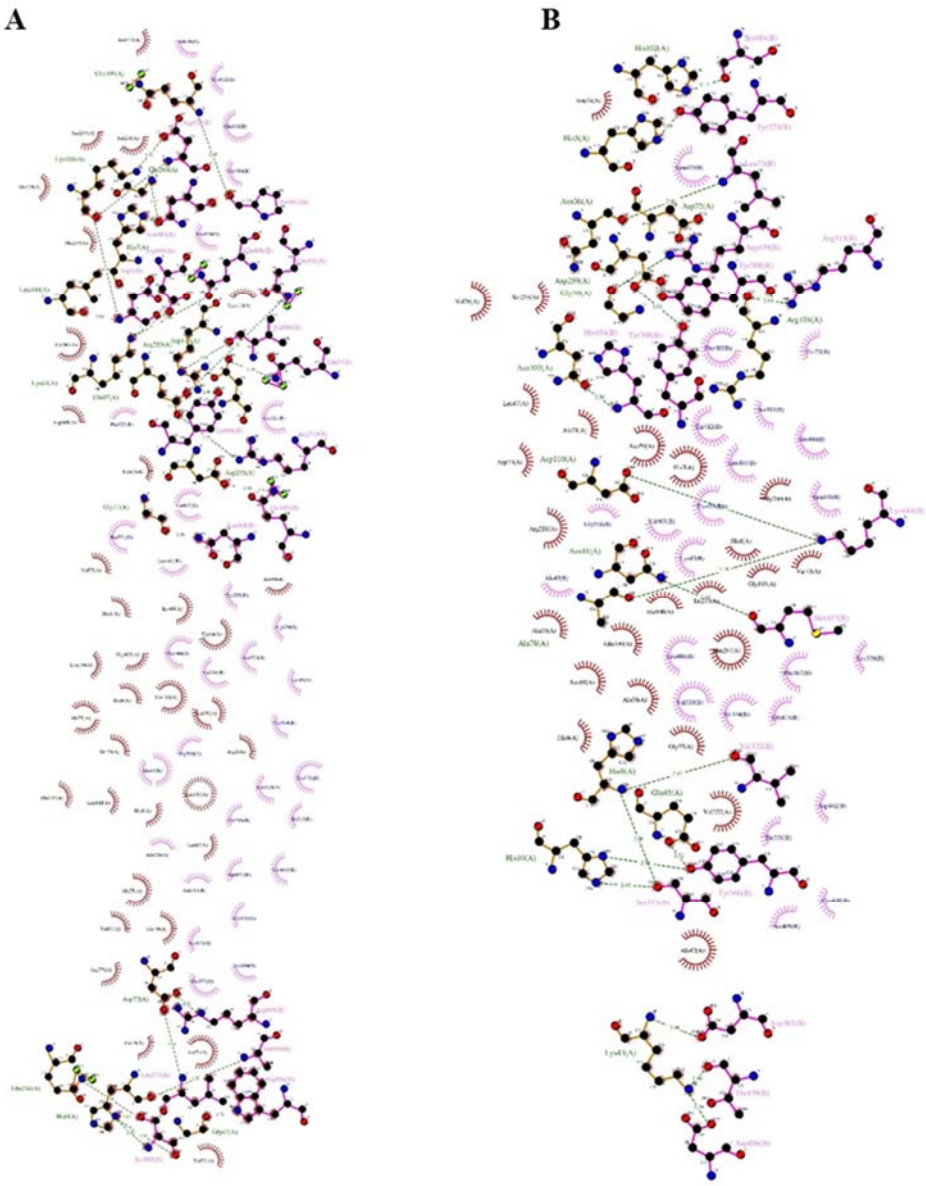

Fig. 4. Two-dimensional representation of protein-protein interactions for the complex (A) DARPin EG3-1 and (B) DARPin EG3-2 binding mode and the position of the hydrogen bonds of the extracellular domain of human epidermal growth factor receptor 2. Dashed green lines indicate hydrogen bonds, and the half-moon indicates hydrophobic interactions**.** DARPin EG, Designed ankyrin repeat proteins engineered G.

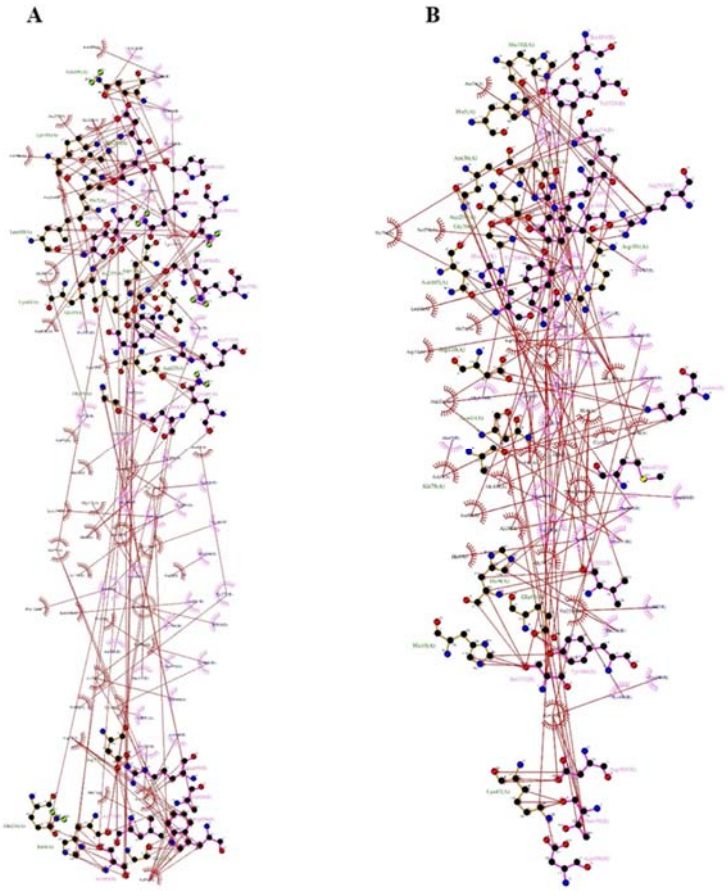

Fig. 5. Two-dimensional representation of protein-protein interactions for the complex (A) DARPin EG3-1 and (B) DARPin EG3-2 binding mode and the position of the hydrophobic bonds of the extracellular domain of human epidermal growth factor receptor 2. DARPin EG, Designed ankyrin repeat proteins engineered G.

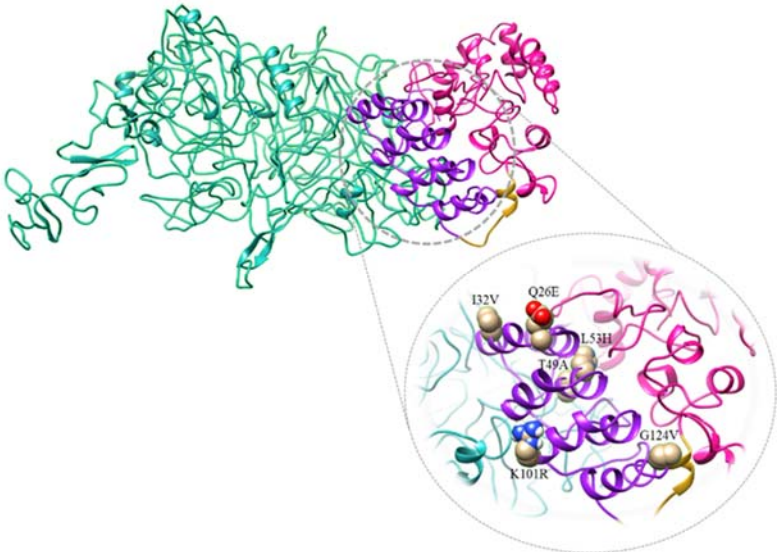

Fig. 6. Structure of the designed DARPin EG3-2 / human epidermal growth factor receptor 2 complex and its mutation site (magnified). Mutated residues in the DARPin EG3-2 variant are represented by gold spheres mode. The DARPin, linker, BAX-Smac, and receptor domains are depicted in purple, gold, magenta, and light sea green, respectively. Image created using Chimera 1.12. DARPin EG, Designed ankyrin repeat proteins engineered G; BAX, Bcl-2-associated X protein; Smac, second mitochondria-derived activator of caspase.

DISCUSSION

Resistance to chemotherapy, metastasis, and disease recurrence is observed in most patients with breast cancer despite common treatments such as radiation therapy, surgery, and chemotherapy (22). With a better understanding of the molecular mechanisms of breast cancer, improved strategies for targeted therapies have been developed recently. Increasing the specificity and affinity of HER2 aptamers and combining them with other therapeutic agents such as drugs, siRNA, apoptosis-inducing proteins, and radionuclides can lead to the development of an effective and efficient drug for treating breast cancer (23-26).

DARPin and its mutations have not been the subject of bioinformatics research until now. In this study, homology modeling was used to create two new EG3-1 (native) and EG3-2 (mutated) DARPins as HER2 receptor targets. The structures were then optimized through molecular dynamic simulation, and their physicochemical properties were assessed. Afterward, they were docked to the ECD domain of the HER2 receptor to select a superior and more appropriate structure for future experimental studies.

MD simulation trajectory analysis for DARPin EG3-1 and EG3-2 revealed the quality of these structures. The small standard deviation of the backbone's RMSD values indicated that both models possessed stable structures, and systems reached equilibrium after approximately 20 ns of MD simulation. The simulation time was sufficient, so the final structures were analyzed further. Comparing the RMSD changes of DARPin EG3-1 and DARPin EG3-2 revealed that the RMSD of EG3-2 (mutated) was 1.3 nanometers greater. The mutation then causes substantial structural changes in DARPin. In addition, RMSF and surface accessibility analyses revealed that DARPin EG3-2 fluctuates less than native DARPin. Few variations in the flexibility of mutation sites in DARPin EG3-2 compared to native DARPin indicate that these mutations had no detrimental effect on the protein's stability. Multiple studies have demonstrated that substituting arginine and hydrophobic residues is an effective method for enhancing protein stability (27-30).

Although Houlihan *et al.* demonstrated that the Q26E, I32V, T49A, L53H, K101R, and G124V mutations increase DARPin's HER2 affinity compared to that of its parent, it remains unclear whether these mutations are causal. Due to the presence of linker, BAX, and Smac in the newly designed DARPin structure, it is necessary to conduct additional computational (and experimental) studies. The results demonstrated that the average number of hydrogen bonds between water and protein in modified DARPin was slightly higher than in native DARPin, indicating that mutations can increase DARPin's solubility (Table 1).

Consistent with RMSF findings, DARPin EG3-2 exhibited less Rg, a more compact structure, less flexibility, and greater stability than native DARPin. According to RMSF plots, local structural fluctuations at mutation sites did not differ significantly between native and mutated variants (residues 26, 32, 49, 53, and 101). Only the G124V substitution in the helix-coil structure of DARPin EG3-2 exhibited a negligible increase in flexibility compared to the native form (about 0.1 nm).

Calculating the average number of secondary structure residues during the last 30 s of MD simulation revealed the effect of mutations on the secondary structure. In the mutated form and its complex with the HER2 receptor, the rigid structural elements, such as β-sheet and α-helix structures, were almost dominant. During the simulation, the flexible structural elements (coils) of the native protein predominated (Table 2). These results indicate that this mutation improved the secondary structure and stability of mutant DARPin.

DARPins bind HER2 *via* domain IV, which can be used as a therapeutic strategy for breast cancer due to their anti-proliferative effect on HER2-overexpressing cells (5). Molecular docking was performed to determine if the enumerated mutations could affect DARPin's affinity for the HER2 IV domain. DARPin EG3-2 had a higher binding affinity and better van der Waals interaction with the HER2 receptor, as determined by docking results (Table 3). The nature of the inserted valine and alanine residues is most likely responsible for the enhanced van der Waals interaction. The more negative desolation energy of DARPin

EG3-2 relative to its native form indicates the more proper removal of water molecules from free proteins, resulting in stronger binding of DARPin EG3-2 to the HER2 receptor. Typically, this energy is a crucial driving force for protein-ligand binding (32).

The molecular interactions of drugs with target proteins and the detailed motion of molecules or atoms during a period can be studied *via* MD simulation (17). The results showed that both complexes reached a stable structure after 20 ns. The trivial standard deviation in RMSD, RMSF, and Rg of both DARPins and HER2 receptors in complexes during the last 50 ns of MD simulation showed that the obtained structures reached a stable structure, and simulation results of complexes were valid.

The sum of van der Waals and electrostatic energies between DARPin EG3-1 and the HER2 receptor complex was more negative than that of between DARPin EG3-2 and the HER2 receptor complex. In addition, the average number of hydrogen bonds between DARPin EG3-2 and HER2 was lower than that of native DARPin in the complex (Table 5). This is most likely due to greater backbone RMSD of HER2 in the EG3-2 complex compared to the EG3-1 complex, resulting in greater structural changes to the initial structure. This conformational change can reduce the number of interactions between EG3-2 and HER2 receptors and raise the total electrostatic and van der Waals energies. In addition, the difference in the number of DARPin atoms between mutated and native DARPin may have influenced the results above.

CONCLUSION

This study aimed to design a novel protein-containing peptide aptamer with greater specificity for the HER2 receptor-bound apoptotic protein. Using homology modeling, docking, and MD simulations, a model for constructing a new DARPin variant with increased affinity was developed to create a more effective breast cancer treatment drug. We analyzed the interaction between an engineered mutant DARPin variant and HER2 due to the importance of their binding in forming a binary complex between DARPin and HER2 for the delivery of targeted drugs to cancer cells. According to molecular docking and MD simulation, DARPin EG3-1 and EG3-2 had the appropriate structure, respectively. Nevertheless, the final course of action depends on examining the affinity and stability of these two structures in the biological environment and cell culture. Finally, these newly designed DARPins have therapeutic potential for breast cancer treatment.

Acknowledgments

The study was financially supported by the Vice-Chancellery of Research of Isfahan University of Medical Sciences, Isfahan, Iran through Grant No. 397775.

Conflict of interest statement

The authors declared no conflict of interest in this study.

Authors' contribution

M. Beheshti Isfahani wrote the article; K. Mahnam conducted the scientific guidance and revised the manuscript; H. Seyedhosseini-Ghaheh contributed to MD simulation analysis and visualization of results; H. Mir Mohammad Sadeghi contributed to article writing and editing; H. Khanahmad, V. Akbari, and J. Varshosaz contributed to article writing and editing. The finalized article was approved by all authors.

REFERENCES

1. Kumar A, Singla A. Epidemiology of breast cancer: current figures and trends. In: Mehta S, Singla A, editors. Preventive oncology for the gynecologist. Singapore: Springer Singapore; 2019. pp. 335-339. DOI: 10.1007/978-981-13-3438-2_26.
2. Bang YJ, Van Cutsem E, Feyereislova A, Chung HC, Shen L, Sawaki A, *et al*. Trastuzumab in combination with chemotherapy versus chemotherapy alone for treatment of HER2-positive advanced gastric or gastro-oesophageal junction cancer (ToGA): a phase 3, open-label, randomised controlled trial. Lancet. 2010;376(9742):687-697. DOI: 10.1016/S0140-6736(10)61121-X.
3. Ahmed N, Brawley VS, Hegde M, Robertson C, Ghazi A, Gerken C, *et al*. Human epidermal growth factor receptor 2 (HER2)-specific chimeric antigen receptor-modified T cells for the immunotherapy of

HER2-positive sarcoma. J Clin Oncol. 2015;33(15):1688-1696.
DOI: 10.1200/JCO.2014.58.0225.
4. Reverdatto S, Burz DS, Shekhtman A. Peptide aptamers: development and applications. Curr Top Med Chem. 2015;15(12):1082-1101.
DOI: 10.2174/1568026615666150413153143.
5. Goldstein R, Sosabowski J, Livanos M, Leyton J, Vigor K, Bhavsar G, *et al*. Development of the designed ankyrin repeat protein (DARPin) G3 for HER2 molecular imaging. Eur J Nucl Med Mol Imaging. 2015;42(2):288-301.
DOI: 10.1007/s00259-014-2940-2.
6. Houlihan G, Gatti-Lafranconi P, Lowe D, Hollfelder F. Directed evolution of anti-HER2 DARPins by SNAP display reveals stability/function trade-offs in the selection process. Protein Eng Des Sel. 2015;28(9):269-279.
DOI: 10.1093/protein/gzv029.
7. Plückthun A. Designed ankyrin repeat proteins (DARPins): binding proteins for research, diagnostics, and therapy. Annu Rev Pharmacol Toxicol. 2015;55:489-511.
DOI: 10.1146/annurev-pharmtox-010611-134654.
8. Stüber JC, Richter CP, Bellón JS, Schwill M, König I, Schuler B, *et al*. Apoptosis-inducing anti-HER2 agents operate through oligomerization-induced receptor immobilization. Commun Biol. 2021;4(1):762,1-12.
DOI: 10.1038/s42003-021-02253-4.
9. Hasenjäger A, Gillissen B, Müller A, Normand G, Hemmati PG, Schuler M, *et al*. Smac induces cytochrome c release and apoptosis independently from Bax/Bcl-xL in a strictly caspase-3-dependent manner in human carcinoma cells. Oncogene. 2004;23(26):4523-4535.
DOI: 10.1038/sj.onc.1207594.
10. Godlewski MM, Gorka M, Lamparska-Przybysz M, Motyl T. Minute kinetics of proapoptotic proteins: BAX and Smac/DIABLO in living tumor cells revealed by homeostatic confocal microscopy. Cytotechnology. 2004;45(3):141-153.
DOI: 10.1007/s10616-004-7255-x.
11. Fulda S. Promises and challenges of Smac mimetics as cancer therapeutics. Clin Cancer Res. 2015;21(22):5030-5036.
DOI: 10.1158/1078-0432.CCR-15-0365.
12. Derakhshan A, Chen Z, Van Waes C. Therapeutic small molecules target inhibitor of apoptosis proteins in cancers with deregulation of extrinsic and intrinsic cell death pathways. Clin Cancer Res. 2017;23(6):1379-1387.
DOI: 10.1158/1078-0432.CCR-16-2172.
13. Lv Z, Song X, Xu J, Jia Z, Yang B, Jia Y, *et al*. The modulation of Smac/DIABLO on mitochondrial apoptosis induced by LPS in Crassostrea gigas. Fish Shellfish Immunol. 2019;84:587-598.
DOI: 10.1016/j.fsi.2018.10.035.
14. Kanwar JR, Shankaranarayanan JS, Gurudevan S, Kanwar RK. Aptamer-based therapeutics of the past, present and future: from the perspective of eye-related diseases. Drug Discov Today. 2014;19(9):1309-1321.
DOI: 10.1016/j.drudis.2014.02.009.
15. Buglak AA, Samokhvalov AV, Zherdev AV, Dzantiev BB. Methods and applications of *in silico* aptamer design and modeling. Int J Mol Sci. 2020;21(22):8420,1-25.
DOI: 10.3390/ijms21228420.
16. Seyedhosseini Ghaheh H, Ganjalikhany MR, Yaghmaei P, Pourfarzam M, Mir Mohammad Sadeghi H. Improving the solubility, activity, and stability of reteplase using *in silico* design of new variants. Res Pharm Sci. 2019;14(4):359-368.
DOI: 10.4103/1735-5362.263560.
17. Payab N, Mahnam K, Shakhsi-Niaei M. Computational comparison of two new fusion proteins for multiple sclerosis. Res Pharm Sci. 2018;13(5):394-403.
DOI: 10.4103/1735-5362.236832.
18. Riggio AI, Varley KE, Welm AL. The lingering mysteries of metastatic recurrence in breast cancer. Br J Cancer. 2021;124(1):13-26.
DOI: 10.1038/s41416-020-01161-4.
19. GA. Jeffrey, W. Saenger. Hydrogen Bonding in Biological Structures. Berlin: Springer-Verlag; 2012. pp. 360-391
20. Cho HS, Mason K, Ramyar KX, Stanley AM, Gabelli SB, Denney DW, *et al*. Structure of the extracellular region of HER2 alone and in complex with the Herceptin Fab. Nature. 2003;421(6924): 756-760.
DOI: 10.1038/nature01392.
21. Pettersen EF, Goddard TD, Huang CC, Couch GS, Greenblatt DM, Meng EC, *et al*. UCSF Chimera-a visualization system for exploratory research and analysis. J Comput Chem. 2004;25(13):1605-1612.
DOI: 10.1002/jcc.20084.
22. Pimentel GC, McClellan AL. Hydrogen bonding. Annua Rev Phys Chem. 1971;22(1):347-385
DOI: 10.1146/annurev.pc.22.100171.002023.
23. Han J, Gao L, Wang J, Wang J. Application and development of aptamer in cancer: from clinical diagnosis to cancer therapy. J Cancer. 2020;11(23):6902-6915.
DOI: 10.7150/jca.49532. eCollection 2020.
24. Vi C, Mandarano G, Shigdar S. Diagnostics and therapeutics in targeting HER2 breast cancer: a novel approach. Int J Mol Sci. 2021;22(11):6163,1-26.
DOI: 10.3390/ijms22116163.
25. Wu X, Shaikh AB, Yu Y, Li Y, Ni S, Lu A, *et al*. Potential diagnostic and therapeutic applications of oligonucleotide aptamers in breast cancer. Int J Mol Sci. 2017;18(9):1851,1-23.
DOI: 10.3390/ijms18091851.
26. Gijs M, Penner G, Blackler GB, Impens NR, Baatout S, Luxen A, *et al*. Improved aptamers for the diagnosis and potential treatment of HER2-positive cancer. Pharmaceuticals (Basel). 2016;9(2):29,1-21.
DOI: 10.3390/ph9020029.
27. Osire T, Yang T, Xu M, Zhang X, Li X, Niyomukiza S, *et al*. Lys-Arg mutation improved the thermostability of *Bacillus cereus* neutral protease

through increased residue interactions. World J Microbiol Biotechnol. 2019;35(11):173,1-11. DOI: 10.1007/s11274-019-2751-5.
28. Islam MM, Kobayashi K, Kidokoro SI, Kuroda Y. Hydrophobic surface residues can stabilize a protein through improved water-protein interactions. FEBS J. 2019;286(20):4122-4134. DOI: 10.1111/febs.14941. Epub 2019 Jun 17.
29. Seyedhosseini Ghaheh H, Sajjadi S, Shafiee F, Barzegari E, Moazen F, Mir Mohammad Sadeghi H. Rational design of a new variant of reteplase with optimized physicochemical profile and large-scale production in *Escherichia coli*. World J Microbiol Biotechnol. 2022;38(2):29. DOI: 10.1007/s11274-021-03204-1.
30. Pal S, Mitra RK. Investigation on the effect of nonpolar amino acids as macromolecular crowders on the stability of globular proteins. Chem Thermodyn Therm Anal. 2022;6:100044,1-6. DOI: 10.1016/ 2022.100044.
31. Dominguez C, Boelens R, Bonvin AM. HADDOCK: a protein-protein docking approach based on biochemical or biophysical information. J Am Chem Soc. 2003;125(7):1731-1737. DOI: 10.1021/ja026939x.
32. Mondal J, Friesner RA, Berne B. Role of desolvation in thermodynamics and kinetics of ligand binding to a kinase. J Chem Theory Comput. 2014;10(12):5696-5705. DOI: 10.1021/ct500584n.

SUPPLEMENTARY MATERIALS

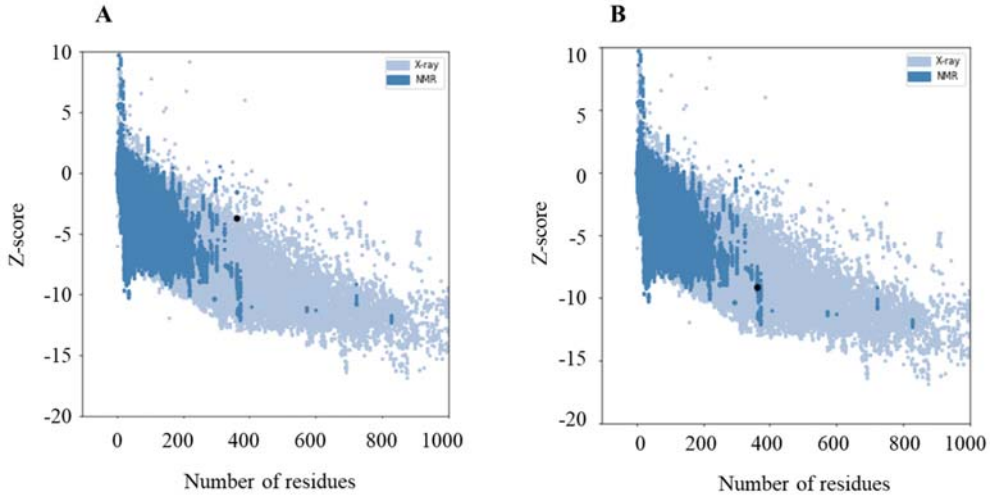

Fig. S1. Prosa web Z-score plots of the best-selected model of engineered (A) G3-1, Z-score = -3.67; (A2) engineered G3-2, Z-score = -9.17.